Equilibrium distribution of Pb between copper metal and slags

T. Kan[1] *and C. Chen*[2]

1.Research Scientist, CSIRO Mineral Resources, Clayton, VIC 3168, Australia. Email: tao.kan@csiro.au
2. Principal Research Scientist, CSIRO Mineral Resources, Clayton, VIC 3168, Australia. Email: chunlin.chen@csiro.au

Keywords: Black copper; E-waste smelting; Lead distribution; Thermodynamic equilibrium; FeO_x–CaO–SiO_2 slag

ABSTRACT

The distribution ratio of Pb ($L_{Pb}^{s/m}$) between three types of slags (FeO_x–SiO_2, CaO–FeO_x and FeO_x–CaO–SiO_2) and molten copper after equilibrium was measured at 1300 °C and oxygen partial pressure (pO_2) of 10^{-10}–10^{-6} atm. Results showed that for FeO_x–SiO_2 slag, the $L_{Pb}^{s/m}$ increased from 0.024 to 2.57 with pO_2 increased from 10^{-10} to 10^{-6} atm. The $L_{Pb}^{s/m}$ with CaO–FeO_x slag was lower than the FeO_x–SiO_2 slag at the same pO_2, ranging between 0.015 and 0.53. Using the FeO_x–CaO–SiO_2 slag generated $L_{Pb}^{s/m}$ values (0.02–1.6) in between. The oxygen partial pressure in the investigated range had no obvious effect on the activity coefficient of PbO (γ_{PbO}) which was averagely 0.44, 1.70 and 0.71 for FeO_x–SiO_2, CaO–FeO_x and FeO_x–CaO–SiO_2 slags, respectively. The increases in the (CaO+MgO)/SiO_2 mass ratio of the FeO_x–CaO–SiO_2 slag induced the decrease in the $L_{Pb}^{s/m}$ and the increase in the γ_{PbO} value. However, the variation in the Fe/SiO_2 mass ratio didn't exert obvious effects.

1. INTRODUCTION

Waste Electrical or Electronic Equipment (WEEE) or electronic waste (e-waste), denoted as 'any type of non-functional and abandoned electrical or electronic equipment', has been one of the fastest growing hazardous waste streams (Nithya, Sivasankari and Thirunavukkarasu, 2021). The global e-waste amount was 53.6 Mt in 2019 with a potential number of more than 70 Mt in 2030; however, only 17.4% of e-waste was recycled formally (Forti et al., 2020; Nithya, Sivasankari and Thirunavukkarasu, 2021). E-waste has a general composition of 65–70 % of metals, ~ 20 wt.% of plastics and ~ 5 wt.% of glass (Babu, Parande and Basha, 2007). It has been deemed as a reservoir of common valuable metals such as Cu, Fe, Al and Ni and less common or trace elements such as Au, Ag, Pt, Sn, Ge and Se (Ebin and Isik, 2016). Metals of concern/hazardous metals (Be, As, Cd, In, Sb, Hg and Pb) may also be present in the e-waste (Hagelüken, Umicore and Co, 2006). For example, Pb can be present in the e-waste with a high content (e.g., 1.3–6.3 wt.% in printed circuit boards) and is generally considered as a deleterious heavy metal with environmental concerns (Chakraborty et al., 2022; Khaliq et al., 2014). Improper handling of e-waste such as landfilling or incineration without suitable pollutant control will exert significant negative effects on the environment (Tian et al., 2021). E-waste recycling and reclamation are an imperative and challenging task for most countries.

E-waste can be processed through pyrometallurgical processes such as primary copper smelting or secondary copper smelting. Secondary copper smelting treats e-waste through different routes involving a number of metallurgical processes, e.g., reduction (at pO_2 of ~ 10^{-10} atm) of copper oxides followed by oxidation (at pO_2 of ~ 10^{-6} atm) of impurities, or vice versa, depending on the copper contents of the secondary materials (Yamasue et al., 2009). Besides the copper recycling, simultaneous recovery of minor elements is also significant. Secondary copper smelting including 'black copper' smelting featuring the utilisation of copper as the valuable metals collector, is still in the preliminary development (Ghodrat et al., 2018). Impurities such as Fe, Pb and As may be removed to the slag phase as oxides with residual amounts reporting to the copper. However, the presence of impurities such as Pb in the copper metal products if not removed will compromise their physical properties and workability. Elements with high volatilisation such as Pb, Sn, Zn and As may also partition to exhaust gas phase. The main fluxing agents are FeO_x, SiO_2 and CaO, forming slag systems of FeO_x-SiO_2 (fayalite slag, briefly F slag) and CaO-FeO_x (calcium ferrite slag, briefly CF slag). The addition of CaO into FeO_x-SiO_2 system to form FeO_x-CaO-SiO_2 (ferrous calcium silicate slag, briefly FCS slag) was also investigated in some studies and industrial practices to gain benefits such as a lower viscosity of slag (Ghodrat et al., 2016; Shuva et al., 2016; Ye, Liu and Xia, 2021). Substantial Al_2O_3 is generally present in the e-waste smelting slag. Other additives such as MgO, B_2O_5 and Na_2O could also be present to alter the slag properties.

In Australia, a significant amount of e-waste is being generated with an estimated number at ~ 22 kg/capita (or 554 kt in total) in 2019 which was much higher than the world average at 6–7 kg/capita (Baldé et al., 2017; Forti et al., 2020). Substantial amounts of e-waste are still not successfully collected and recycled. The associated revenue potential from recoverable metals and other materials was estimated as 3.59 billion US$ in 2015 in Australia (Islam and Huda, 2019). In Australia, only a few primary smelters are in commission currently, i.e., BHP Billiton's Olympic Dam flash smelter in South Australia and Glencore's Mt Isa top submerged lance (TSL) bath smelter in Queensland which are remote from cities where e-waste collection takes place (Islam, Haque and Somerville, 2021).

Extensive research has been done on the thermodynamic behaviour of impurities originating from the primary copper concentrate materials. Gaining more thermodynamic knowledge about recycling or removing impurities from secondary resources such as e-waste is of high interest (Khaliq et al., 2014; Shuva et al., 2016). The published data with focus on thermodynamics of Pb in secondary copper smelting (e.g., black copper smelting) is still limited and needs further investigation (Shuva et al., 2016). In the meantime, discrepancies in Pb data are found in previous studies (Sineva et al., 2021). The obtained new data in this study is expected to bridge the gap of some existing data. In this study, experiments were carried out at T = 1300 °C and pO_2 of 10^{-10}–10^{-6} atm to simulate the black copper smelting processes. The effects of oxygen partial pressure, different slag systems (F, CF and FCS slags), and composition of FCS slag with varied $(CaO+MgO)/SiO_2$ (taking into account of dissolved MgO from crucibles) and Fe/SiO_2 ratios on the thermodynamic behaviour of Pb were investigated.

2. EXPERIMENTAL

The master copper-lead alloy was first prepared by adding around 1 wt.% of Pb metal to molten copper in a magnesia crucible at 1150 °C in inert N_2 in an induction furnace. Afterwards, a silica tube was used to suck the molten alloy which was then collected after cooling down. The F, CF and FCS master slags were prepared in magnesia crucibles from analytical reagents, i.e., Fe_3O_4 with SiO_2, $CaCO_3$ with Fe_3O_4, and Fe_3O_4 with $CaCO_3$ and SiO_2, respectively. FCS slags with varied CaO/SiO_2 and Fe/SiO_2 ratios were also proposed.

FIG 1 shows the schematic diagram of the experimental setup. The equilibrium experiments were performed in a vertical tube furnace equipped with an alumina tube and water-cooled end-caps. A refractory platform with an inserted thermocouple from the bottom was placed in the hot zone inside the alumina tube.

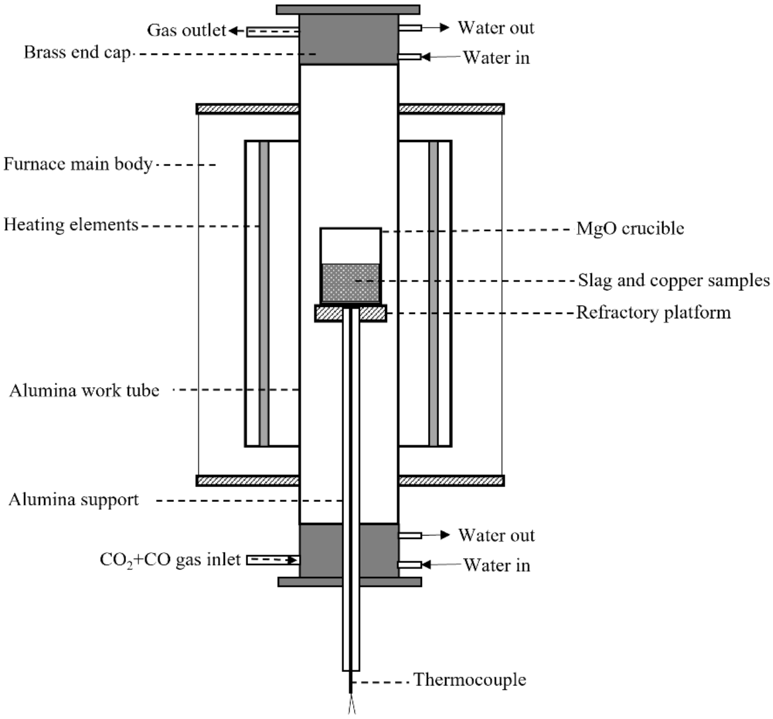

FIG 1 – Schematic diagram of vertical tube furnace with slag-copper equilibrium experimental setup.

The hot zone was preheated to 1300 °C and kept at this temperature. In each run, around 5 g of copper alloy and 5 g of master slag were placed in a magnesia crucible which was then mounted onto the platform from the top of the alumina tube. Magnesia crucibles were used for reasons. This study aimed to investigate the F, CF and FCS slags without the addition of other additives such as alumina which is although more likely to be present in industrial e-waste smelting slags. In the meantime, the magnesia crucible is highly resistant to the attack from slags. The addition of alumina and/or other additives into slags, or the use of alumina crucible, has been considered in the next stage of the study. CO and CO_2 mixture gas at a specified flowrate ratio was introduced into the tube to maintain the desired pO_2 (10^{-10} to 10^{-6} atm) based on Eq. 1 and Eq. 2 (Yazawa and Takeda, 1982).

$$2CO\ (g) + O_2\ (g) = 2CO_2\ (g) \qquad \text{(Eq. 1)}$$

$$\log \mathrm{pO2}\ (\mathrm{atm}) = 2\log\left(\frac{pCO_2}{pCO}\right) - \frac{29510}{T} + 9.05 \qquad \text{(Eq. 2)}$$

The samples were maintained at 1300 °C in a desired pO_2 (10^{-10} to 10^{-6} atm) continuously for 20 hours for complete equilibration. Afterwards, the hot crucible was removed and quenched in cold water promptly. The obtained slag and copper phases were separated physically after drying. The slag was crushed to less than 210 µm and the contained copper droplets were removed carefully. Subsequently, the slag particles were ground manually to less than 45 µm before being analysed. Elemental compositions of slag and copper samples were tested through acid digestion followed by ICP-OES (model: Agilent 5900) and ICP-MS (model: Agilent 8900). The contents of Fe, Ca and Si in the slag were tested by XRF with fused bead method.

3. RESULTS AND DISCUSSION

3.1. Pb distribution ratio with oxygen partial pressure

The distribution of a minor element (Pb in this study) between slag and copper phases can be simply described by the following Eq. 3:

$$[Pb] + \upsilon/2O_2 = (PbO_\upsilon) \qquad \text{(Eq. 3)}$$

where [ ] = value in copper phase, ( ) = value in slag phase, and 2υ = valence state of Pb in slag.

This reaction is commonly described as below (Takeda, Ishiwata and Yazawa, 1983):

$$Pb\ (l) + \tfrac{1}{2}O_2\ (g) = PbO\ (l) \qquad \Delta G^\circ = -195100 + 77.7T\ (J/mol) \qquad \text{(Eq. 4)}$$

The equilibrium constant K can be defined in Eq. 5:

$$K = \alpha_{PbO\upsilon/(}\alpha_{Pb}{*}P_{O_2}^{\upsilon/2}) \qquad \text{(Eq. 5)}$$

where $\alpha_{PbO\upsilon}$ = activity of PbO_υ in slag and α_{Pb} = activity of Pb in copper.

Also, K can be calculated based on the following Eq. 6 and the obtained ΔG° from Eq. 4.

$$\Delta G^\circ = -RT\ \ln K \qquad \text{(Eq. 6)}$$

The distribution ratio of Pb ($L_{Pb}^{s/m}$) between slag (s) and copper metal (m) is defined as the mass percentage of Pb in slag divided by its mass percentage in copper metal as below:

$$L_{Pb}^{s/m} = \frac{(Pb\%)}{[Pb\%]} = \frac{K(n_T)[\gamma_{Pb}]\ P_{O_2}^{\upsilon/2}}{[n_T]\ (\gamma_{PbO\upsilon})} \qquad \text{(Eq. 7)}$$

where n_T = total number of moles in constituents in 100 g of each phase,

γ_{Pb} is the activity coefficient of Pb in metal, and

$\gamma_{PbO\upsilon}$ is the activity coefficient of PbO_υ in slag.

The activity coefficient of PbO_{υ} in slag can be calculated according to:

$$\gamma_{PbO\upsilon} = \frac{K(n_T)[\gamma_{Pb}]\ P_{O_2}^{\upsilon/2}}{[n_T]\ L_{Pb}^{s/m}} \qquad \text{(Eq. 8)}$$

where $[\gamma_{Pb}] = 4.8$ is used in this study (Kaur, Swinbourne and Nexhip, 2009; Shuva et al., 2016).

The experimental results as well as the calculated $L_{Pb}^{s/m}$ and $\gamma_{PbO\upsilon}$ are summarised in Table 1.

TABLE 1 – List of experiments and analysis results of slag and copper after equilibrium.

ID	Slag	pO_2 (atm)	Slag composition (wt.%)						Pb (mg/kg)		(CaO+MgO) /SiO_2	Fe/SiO_2	$L_{Pb}^{s/m}$	γ_{PbO}
			FeO	Fe_2O_3	CaO	SiO_2	MgO	Cu	Slag	Copper alloy				
F-O2(-6)	FeO_x-SiO_2	10^{-6}	35.89	16.59	0.24	25.78	11.79	5.22	3600	1400	NC	NC	2.57	0.45
F-O2(-7)	FeO_x-SiO_2	10^{-7}	37.44	16.62	0.20	27.20	11.92	4.30	1700	1200	NC	NC	1.42	0.27
F-O2(-8)	FeO_x-SiO_2	10^{-8}	48.50	8.38	0.10	27.77	10.54	1.73	1100	3600	NC	NC	0.31	0.40
F-O2(-9)	FeO_x-SiO_2	10^{-9}	50.69	8.02	0.12	27.49	9.92	0.82	340	5400	NC	NC	0.06	0.61
F-O2(-10)	FeO_x-SiO_2	10^{-10}	54.42	5.51	0.09	28.67	8.61	0.50	180	7400	NC	NC	0.02	0.50
CF-O2(-6)	CaO-FeO_x	10^{-6}	18.65	47.24	18.43	0.30	3.69	5.35	640	1200	NC	NC	0.53	1.92
CF-O2(-7)	CaO-FeO_x	10^{-7}	26.37	39.49	18.28	0.33	6.28	2.95	410	2700	NC	NC	0.15	2.25
CF-O2(-8)	CaO-FeO_x	10^{-8}	32.16	34.94	19.51	0.28	5.11	2.12	270	4900	NC	NC	0.06	1.99
CF-O2(-9)	CaO-FeO_x	10^{-9}	40.14	28.54	19.71	0.26	4.72	1.35	140	6400	NC	NC	0.02	1.61
CF-O2(-10)	CaO-FeO_x	10^{-10}	48.12	21.51	20.04	0.27	4.38	0.97	39	2600	NC	NC	0.02	0.75
FCS-a-(-6)	CaO-FeO_x-SiO_2	10^{-6}	19.30	8.15	13.95	37.77	13.89	3.81	2400	1500	0.74	0.55	1.60	0.80
FCS-a-(-7)	CaO-FeO_x-SiO_2	10^{-7}	19.43	9.15	14.51	38.37	12.80	2.39	1700	2500	0.71	0.56	0.68	0.60
FCS-a-(-8)	CaO-FeO_x-SiO_2	10^{-8}	23.80	6.83	14.97	39.87	10.96	1.40	1000	4800	0.65	0.58	0.21	0.62
FCS-a-(-9)	CaO-FeO_x-SiO_2	10^{-9}	26.50	4.24	15.15	40.58	11.10	0.75	260	5600	0.65	0.58	0.05	0.90
FCS-a-(-10)	CaO-FeO_x-SiO_2	10^{-10}	27.79	2.50	15.80	40.66	10.51	0.54	140	7000	0.65	0.57	0.02	0.66
FCS-b	CaO-FeO_x-SiO_2	10^{-8}	23.54	6.82	20.65	34.80	10.93	1.09	490	4900	0.91	0.66	0.10	1.31
FCS-c	CaO-FeO_x-SiO_2	10^{-8}	20.71	10.88	29.00	27.63	8.64	0.92	320	7600	1.36	0.86	0.04	3.07
FCS-d	CaO-FeO_x-SiO_2	10^{-8}	28.43	8.21	15.58	34.00	10.20	1.40	620	4400	0.76	0.82	0.14	0.91
FCS-e	CaO-FeO_x-SiO_2	10^{-8}	29.72	11.66	15.42	27.96	11.04	1.19	520	5700	0.95	1.12	0.09	1.38

NC: not calculated.

Rearranging Eq. 5 produces the following:

$$\log L_{Pb}^{s/m} = \log \frac{\mathrm{K}\ (\mathrm{n_T})[\gamma_{Pb}]}{[\mathrm{n_T}]\ (\gamma_{PbO_\upsilon})} + \frac{\upsilon}{2} \log \mathrm{pO2} \qquad \text{(Eq. 9)}$$

The logarithmic plot between $L_{Pb}^{s/m}$ and pO_2 will give a straight line with a slope of υ/2, which will indicate the oxidation state of Pb in the slag. As shown in FIG 2, the Pb distribution ratio was plotted against the oxygen partial pressure over the range of 10^{-10} to 10^{-6} (i.e., log pO_2 of -10 to -6) atm for F slag-copper, CF slag-copper and FCS slag-copper equilibrium systems. The data of previous studies on these three slag systems was also exhibited in each sub-figure for comparison.

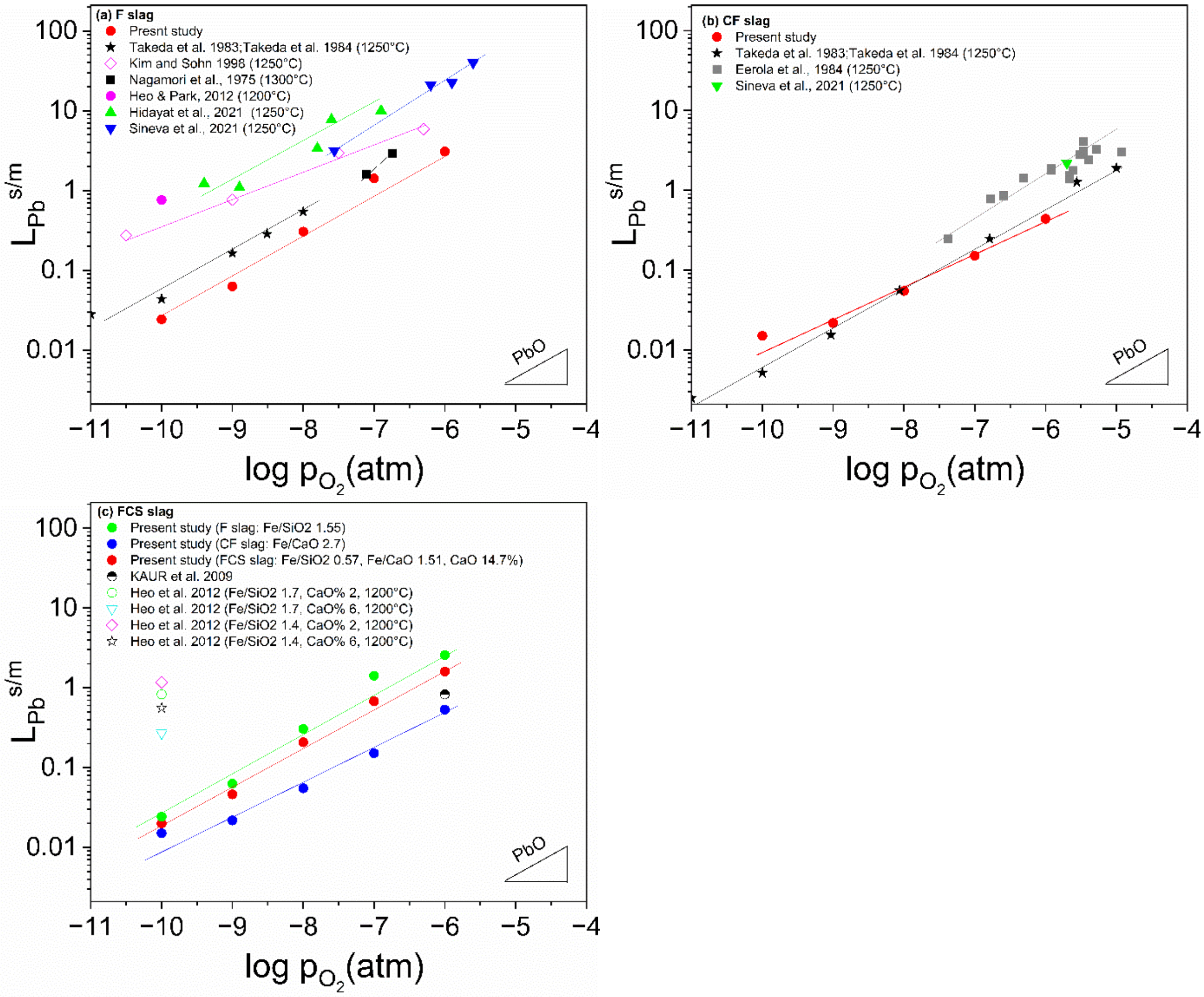

FIG 2 – Pb distribution ratio with oxygen partial pressure.

The distribution ratio of Pb generally relies on several parameters such as properties of the element itself, slag composition, oxygen partial pressure and temperature. In present study using F slag, the $L_{Pb}^{s/m}$ value was very low (0.024) at $pO_2 = 10^{-10}$ atm and climbed to 3.08 at $pO_2 = 10^{-6}$ atm. Pb preferentially dissolved into copper at $pO_2 < 10^{-7}$ atm while Pb mostly reported to slag ($L_{Pb}^{s/m} > 1$) at $pO_2 > 10^{-7}$ atm. At a higher pO_2, the Pb oxidation reaction (Eq. 3) moves rightwards to form more Pb oxide. Compared to Cu, Pb is more reactive with oxygen to form stable PbO in slag at increased pO_2, thus can be separated from copper phase into slag (Ghodrat et al., 2018). Being similar to previous studies, a linear relationship between log $L_{Sn}^{s/m}$ and log pO_2 was obtained with a slope (υ/2) of 0.5 as an indicator for the bivalence of lead (i.e., PbO). As the figure shows, the $L_{Pb}^{s/m}$ values among most previous studies were inconsistent. The results in this study were close to the data from studies by Nagamori, Mackey and Tarassoff (1975) and Takeda, Ishiwata and Yazawa (1983) which adopted Al_2O_3 and SiO_2 crucible, respectively. Heo & Park (2012) used Al_2O_3 crucible to obtain an average $L_{Pb}^{s/m}$ value of 0.76 at $pO_2 = 10^{-10}$ atm and a low temperature of 1200 °C. Recently, Hidayat et al. (2021) and Sineva et al. (2021) investigated the equilibrium thermodynamics of Pb in in a sealed silica ampoule to minimise the vaporization of Pb, and used tridymite and Fe_3O_4 spinel materials respectively rather than crucibles, acquired much higher $L_{Pb}^{s/m}$ values than this study. Compared to previous studies, the $L_{Pb}^{s/m}$ value in this study was lower to different extents, suggesting that Pb was more likely to retain in the copper at the same oxygen partial pressure. The discrepancy could arise from the variation in slag composition and experimental conditions among various studies. In present study MgO crucibles were used while in previous studies SiO_2 crucibles were mostly employed with a few studies using Al_2O_3 crucible or Fe_3O_4 substrate wrap (see Table 2). In the meantime, in most previous studies equilibration experiments were conducted at the temperature of 1250 °C, which is lower than 1300 °C for this study. Generally, a lower temperature can increase the K value (see Eq. 7) thus increase the $L_{Pb}^{s/m}$ value and promote Pb to move into the slag phase (Chen et al., 2021; Taskinen and Avarmaa, 2021). In the meantime, the slag in this study could contain solids such as olivine, decreasing the concentration of Pb in the slag and therefore the $L_{Pb}^{s/m}$ values.

For Pb distribution between the CF slag and copper, data from this study ranged within 0.02 to 0.44, which is significantly lower than that with F slag. PbO is well recognised as an alkaline compound and is inclined to combine with the acidic SiO_2 in the F slag to generate stable compounds like $PbO\cdot SiO_2$ and $2PbO\cdot SiO_2$, therefore producing much higher $L_{Pb}^{s/m}$ values than those with the CF slag (Kuxmann and Fischer, 1974). The data in present study is in good agreement with that by Takeda, Ishiwata and Yazawa (1983). Higher $L_{Pb}^{s/m}$ values were observed in studies by Eerola, Jylha and Taskinen (1984) and Sineva et al. (2021). However, the difference between these two studies and the present one is not significant.

All the $L_{Pb}^{s/m}$ values with F, CF and FCS slags were plotted in the same sub-figure FIG 2-(c) FCS slag for comparison. FCS slag combines the benefits of both F and CF slags CF slags, giving medium $L_{Pb}^{s/m}$ values between 0.02 ($pO_2 = 10^{-10}$ atm) and 1.6 ($pO_2 = 10^{-6}$ atm) as expected. So far, limited work has been reported on the thermodynamic behaviour of Pb in FCS slag–copper system. Takeda and Yazawa (1989) reported that the lead solubility to slag (log %Pb in slag) increased with the oxygen partial pressure linearly at 1300 °C. Kaur, Swinbourne and Nexhip (2009) obtained a $L_{Pb}^{s/m}$ value of 0.93 at 1300 °C and $pO_2 = 10^{-6}$ atm in MgO crucible. Both the experimental conditions and the $L_{Pb}^{s/m}$ value are in line with the present study. Heo and Park (2012) employed FCS slags with 2–6% CaO at 1200 °C and $pO_2 = 10^{-10}$ atm to gain $L_{Pb}^{s/m}$ values higher than the present study. This could be due to the lower CaO content of FCS slag and lower temperature, compared to the present study (avg. 14.7% CaO in slag and 1300 °C).

In the industrial practice, it is significant to separate Pb from copper to slag as much as possible. The Pb content in cathode copper of higher than a few ppm will produce negative effects such as copper cracking during casting and hot rolling as well as the annealability of copper (Davenport et al., 2002). According to the above observations in the present study, the distribution ratio of Pb between slag and copper was significantly larger in F slag than in CF slag under continuous converting conditions (1300 °C and ~ 10^{-6} atm) in the black copper process. The high risk of slag foaming and other disadvantages related to the F slag should be handled properly. The results suggest FCS slag could be a suitable replacement for F slag due to its improved properties and similar $L_{Pb}^{s/m}$ values in comparison to F slag. The resultant decrease in the impurity level (e.g., Pb) of the black copper will benefit to the enhanced concentration of copper and precious metals with higher stability. However, the loss of Cu in slag as Cu_2O will also increase simultaneously which needs to be taken into account. Undering the reducing smelting conditions (1300 °C and ~ 10^{-10} atm), similar $L_{Pb}^{s/m}$ values for all three slags at low levels were obtained.

3.2. Activity coefficient of PbO

The activity coefficient of PbO (γ_{PbO}) in all three slags versus log pO_2 is calculated based on Eq. 8 then exhibited in FIG 3.

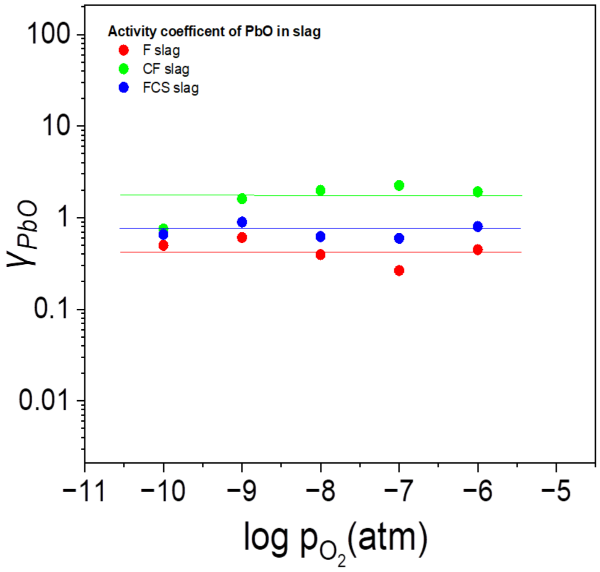

FIG 3 – Activity coefficient of PbO with oxygen partial pressure.

In the present work, the γ_{PbO} value in three slags was not obviously affected by the pO_2. This trend was in good agreement with most previous studies. For the F slag, Nagamori, Mackey and Tarassoff (1975) and Takeda, Ishiwata and Yazawa (1983) obtained a constant γ_{PbO} value of 0.07 and 0.4, respectively. The value in the present study (0.44) was in good accord with that from Takeda, Ishiwata and Yazawa (1983). Both of these two previous studies came to the same conclusion that the γ_{PbO} value was independent of pO_2. Instead, the γ_{PbO} value relies on the properties of both PbO and slag. However, Kim and Sohn (1998) observed that the γ_{PbO} value (0.01–0.1) increased with the increase in pO_2 and explained that 'a strong dependence of γ_{PbO} on pO_2 or even the presence of atomic Pb in iron silicate slag, might not be ruled out at low oxygen potentials (especially below 10^{-10} atm)'.

In terms of the CF slag, a constant γ_{PbO} value versus pO_2 was also observed by previous studies. Takeda, Ishiwata and Yazawa (1983) obtained the value of 3.2 and found it increased with the increase in the CaO content of slag. The same research team investigated the CF slag with molar ratios of FeO_x/(nCaO+nMgO+nFeO_x) at 0.7 and 0.84, and obtained a γ_{PbO} value of 4.0 and 2.0, respectively (Takeda and Yazawa, 1989). A lower value from present study (avg. 1.70) was in line with the value of 1.7±0.6 by Eerola, Jylha and Taskinen (1984).

Regarding the FCS slag, Takeda and Yazawa (1989) studied the Pb distribution at varied slag composition with molar ratios of Q = (nCaO+nMgO)/(nCaO+nMgO+nSiO_n) and R = nFeO_x/(nCaO+nMgO+nSiO_n+nFeO_x). The γ_{PbO} value was 0.3–0.5 (Q = 0.1, R = 0.5–0.8) and 3.0–

1.0 (Q = 0.55, R = 0.2–0.6), respectively. Kaur, Swinbourne and Nexhip (2009) acquired a γ_{PbO} value of 1.4 at 1300 °C and $pO_2 = 10^{-6}$ atm. The γ_{PbO} value in present study was 0.71 which was of the same order of magnitude as those in previous studies.

The γ_{PbO} value was calculated to be in the order of CF slag (avg. 1.70) > FCS slag (avg. 0.71) > F slag (avg. 0.44). Obviously, the acidic F slag showed the strongest affinity to PbO thus decreased it activity coefficient while the CaO component in the CF slag could provide more basicity and weaken the ability of CF slag to dissolve the PbO.

Beside the data of previous studies in sections 3.1 and 3.2, Table 2 more comprehensively summarises previous studies on Pb distribution in various slag-copper systems to give an overall picture of experimental conditions and key findings. Beside the F, CF and FCS slag systems, other slag systems including CaO-SiO_2-Al_2O_3 (Matsuzaki et al., 2000) and SiO_2-CaO-Al_2O_3-MgO-FeO (Botor, Czernecki and Zajączkowski, 2000) were also attempted to equilibrate the copper phase. The γ_{PbO} value increased with increasing the slag basicity (X_{CaO}/X_{SiO2}). From Table 2, it can be seen that there is an disagreement on the effect of Al_2O_3 addition in slag on the behaviour of Pb. Nagamori, Mackey and Tarassoff (1975) found a higher content of Al_2O_3 lowered the γ_{PbO} value while Kim and Sohn (1998) confirmed that distribution behaviour of Pb was not significantly affected by a small amount of Al_2O_3 addition. Heo and Park (2012) observed that the $L_{Pb}^{s/m}$ changed with the Al_2O_3 content of slag without a clear trend however.

TABLE 2 – Summary of previous studies on thermodynamic behaviour of Pb in various slag-copper systems.

Slag system	**Slag composition**	**Crucible**	**log** pO_2**/atm**	**T/◦C**	$L_{Pb}^{s/m}$	γ_{PbO}	**Findings/notes**	**Ref.**
F slag								
FeO_x-SiO_2-(Al_2O_3)	Fe/SiO_2 = 1.51 (or 1.97), Al_2O_3 8.5±0.2% (or 24.5±2.5%)	Al_2O_3	-7.1 to -6.7 (or -9.1 to -7.7)	1300	1.6 to 2.9 (or 4.5-1.7)	0.07	Fe/SiO_2 didn't obviously affect γ_{PbO}. Higher content of Al_2O_3 lowered γ_{PbO}. The γ_{PbO} was independent of pO_2 and T.	Nagamori, Mackey and Tarassoff (1975)
FeO_x-SiO_2	/	SiO_2	-11.5 to -8	1250	0.021 to 0.544	0.4	Constant γ_{PbO} value within Log pO_2/atm = -10 to -7	Takeda, Ishiwata and Yazawa (1983); Takeda, Ishiwata and Yazawa (1984)
FeO_x-SiO_2-(CaO/Al_2O_3/MgO)	Pre-melted slag (58.8% FeO, 5.2% Fe_2O_3 and 36.0% SiO_2) with or without CaO/Al_2O_3/MgO	SiO_2	-12 to -6.3	1250	0.085 to 5.89	0.01-0.1	Distribution behaviour of Pb was not significantly affected by small additions of CaO, Al_2O_3, MgO, or a mixture thereof. The γ_{PbO} increased with increase in pO_2.	Kim and Sohn (1998)
FeO_x-SiO_2-(Al_2O_3)	Fe/SiO_2 = 1.3/1.5, Al_2O_3% = 2–6%	MgO or SiO_2	-10	1200	Avg. 0.76	/	$L_{Pb}^{s/m}$ changed with Al_2O_3 content; however, the trend was not clear.	Heo and Park (2012)
FeO_x-SiO_2 with tridymite	FeO 60%, SiO_2 37% (tridymite 0.02–0.2%)	SiO_2	-9.4 to -6.9	1250	1.1–10	/	Higher concentration of Pb was found in slag than in copper.	Hidayat et al. (2021)
FeO_x-SiO_2	FeO 56±5%, SiO_2 29±2%	Fe_3O_4 (spinel) substrate	-7.6 to -5.6	1250	3.2 to 39.8	/	Experiments were undertaken in a closed system at relatively high oxidising conditions typical for copper refining. Results were in agreement with prediction.	Sineva et al. (2021)
CF slag								
CaO-FeO_x	CaO 20–32%	MgO	-11 to -5	1250	0.0025 to 1.91	3.2	$L_{Pb}^{s/m}$ decreased with increased CaO content of slag. The γ_{PbO} increased with increase in CaO content.	Takeda, Ishiwata and Yazawa (1983); Takeda, Ishiwata and Yazawa (1984)

CaO-FeO_x	Composition of primary slag: 25% CaO, 60% Fe_2O_3 and 15% FeO	CaO	-7.4 to -4.6	1250	0.25 to 3.1	1.7±0.6	No oxygen partial pressure dependence was found for γ_{PbO}.	Eerola, Jylha and Taskinen (1984)
CaO-FeO_x (saturated with MgO)	Composition with different values of R = Fe/(Fe+Ca+Mg)	MgO	-12 to -5	1300	/	4.0 (R = 0.7); 2.0 (R = 0.84)	Equilibrium experiments between slag and Pb metal	Takeda and Yazawa (1989)
CaO-FeO_x	$FeO_{1.5}$ 63.7%, CaO 23.5%	$Ca_2Fe_2O_5$ substrate	-5.7	1250	2.2	/	Pb distribution among copper, slag and solid phases (Fe_3O_4 spinel or $Ca_2Fe_2O_5$) was analysed.	Sineva et al. (2021)
FCS slag								
FeO_x-CaO-SiO_2 (saturated with MgO)	Composition with different values of Q = (Ca+Mg)/(Ca+Mg+Si) and R = Fe/(Fe+Ca+Mg+Si)	MgO	-12 to -5	1300	/	0.3 or 0.5 (Q = 0.1, R = 0.5 or 0.8); 3.0 or 1.0 (Q = 0.55, R = 0.2 or 0.6)	Equilibrium experiments between slag and Pb metal. The solubility of Pb is affected by the activity of SiO_2.	Takeda and Yazawa (1989)
FeO_x-CaO-SiO_2(-Cu_2O)	35% total Fe, 18% SiO_2, 26% CaO and 4% Cu_2O (master slag)	MgO	-6	1300	0.93	1.4	For Pb deportment, replacing CF slag with FCS slag will not produce negative effects during copper converting.	Kaur, Swinbourne and Nexhip (2009)
FeO_x-CaO-SiO_2	Fe/SiO_2 = 1.7 (or 1.4), CaO 2–6%	MgO or SiO_2	-10	1200	0.83–0.27 (or 1.17–0.56)	/	$L_{Pb}^{s/m}$ decreases with increasing CaO content (~6 wt.%) irrespective of Fe/SiO_2 ratio (1.4 to 1.7).	Heo and Park (2012)
FeO_x-SiO_2-CaO-Al_2O_3	Fe/SiO_2 = 0.8–1.4 FeO_x 32.71 wt.% CaO 17.35 wt.% Al_2O_3 6.83 wt.% MgO 2.21 wt.%	TSL	Not reported	1280 ±50	/	/	Partitioning of Pb in slag/copper/dust = 13.8%/9.5%/76.7%	Ye, Liu and Xia (2021)
Other slags								

SiO_2-CaO-Al_2O_3-MgO-FeO	CaO 18.72 SiO_2 46.72 Al_2O_3 16.14 MgO 11.42 Fe_2O_3 7.15	Al_2O_3	$3 \cdot 10^{-11}$ to $2.42 \cdot 10^{-7}$	1400	0.009–0.24	/	Two separate slag phases could occur at $pO_2 > 10^{-8}$ atm.	Botor, Czernecki and Zajączkowski (2000)
CaO-SiO_2-Al_2O_3	$X_{CaO}/X_{SiO2} = 0.5–1.3$	Al_2O_3	-11.5 to -6	1350	0.03–4.0 ($X_{CaO}/X_{SiO2} = 0.77 \pm 0.6$)	0.06–1.03	Lead existed in slag as PbO at $pO_2 = 10^{-10} – 10^{-6}$ atm and Pb_2O at $pO_2 < 10^{-10}$ atm. The γ_{PbO} increased with increasing slag basicity (X_{CaO}/X_{SiO2}).	Matsuzaki et al. (2000)

3.3. Effects of $(CaO+MgO)/SiO_2$ and Fe/SiO_2 mass ratios in slag

The thermodynamic behaviour of minor elements during the black copper smelting process is highly dependent on the slag composition. FIG 4 shows the effects of $(CaO+MgO)/SiO_2$ and Fe/SiO_2 mass ratios in slag on the Pb distribution ratio and activity coefficient of PbO. It is noteworthy that the MgO was from the crucible and included into the calculation of basicity degree of the slag.

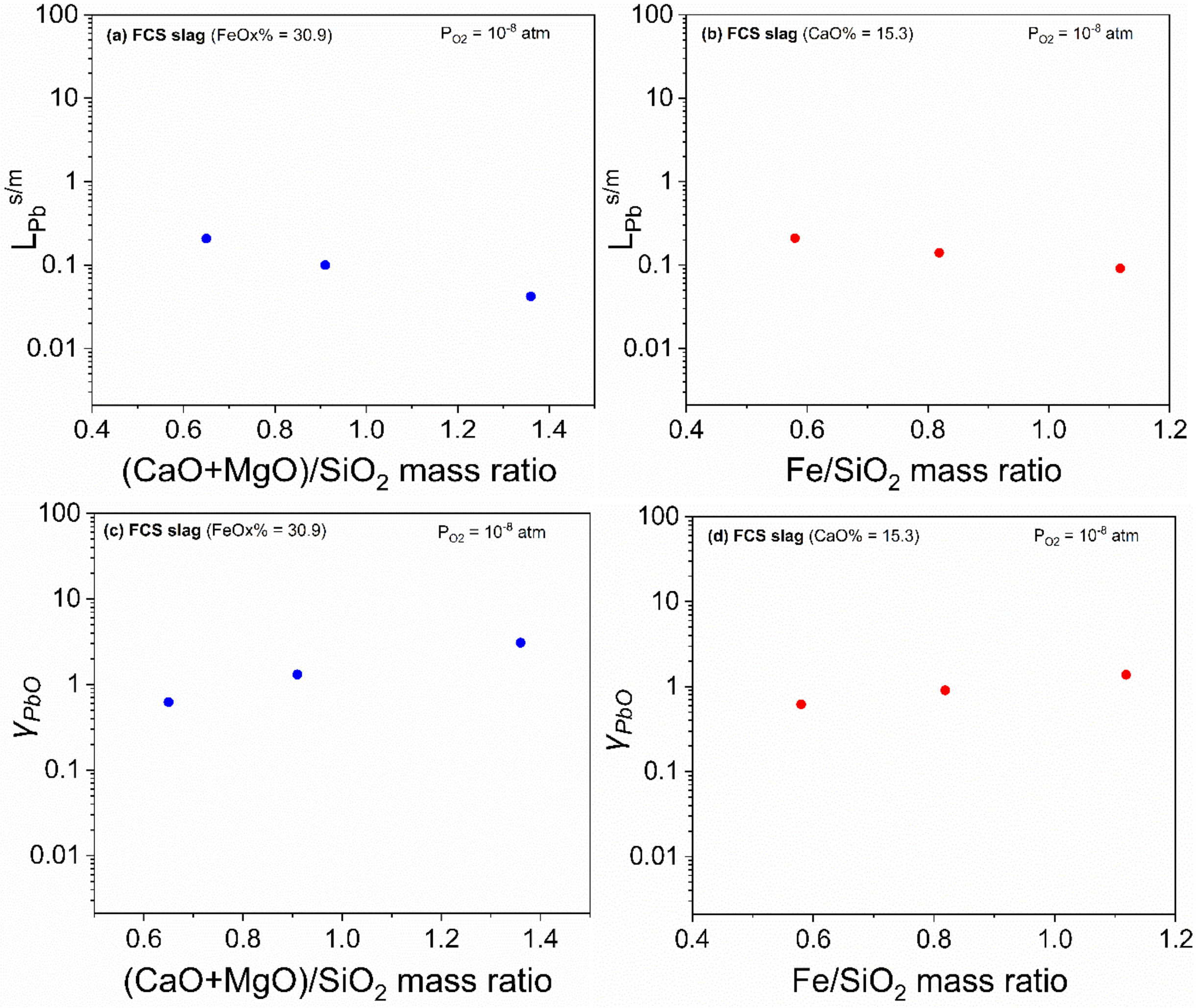

FIG 4 – Effects of $(CaO+MgO)/SiO_2$ and Fe/SiO_2 mass ratios on Pb distribution ratio and activity coefficient of PbO in slag.

In industrial practices, the slag composition is carefully designed to regulate the distribution of elements between slag and copper which is reflected by the activity coefficient of elements with high relevance to the slag composition (Nakajima et al., 2011). When increasing the CaO content in the slag as indicated by the rising $(CaO+MgO)/SiO_2$ ratio, SiO_2 was gradually neutralised by the added CaO with a declining absorbing ability towards PbO. Thus, a decreasing $L_{Pb}^{s/m}$ value with increased $(CaO+MgO)/SiO_2$ mass ratio was observed. An increasing γ_{PbO} with rising $(CaO+MgO)/SiO_2$ mass ratio was determined. The γ_{PbO} value is governed by the interactions between CaO and SiO_2, and between PbO and SiO_2 (Takeda and Yazawa, 1989). Results from

Takeda and Yazawa (1989) indicated that γ_{PbO} increased with the increase in the total content of CaO and MgO in the FeO_n-CaO-SiO_2 slag system in magnesia crucible at 1300 °C.

In the present work, the Fe/SiO_2 mass ratio had no obvious effects on the $L_{Pb}^{s/m}$ and γ_{PbO} (averagely 0.97) within the Fe/SiO_2 range of 0.6–1.1. Nagamori, Mackey and Tarassoff (1975) observed that the γ_{PbO} did not show obvious change for two F slags with Fe/SiO_2 = 1.51 and 1.97 at 1300 °C. In a modelling study, the γ_{PbO} value was constant in FCS slags of varied Fe/SiO_2 ratios with a fixed CaO content (Yazawa, 1994). However, the increase in the Al_2O_3 addition into F slag will lower the γ_{PbO} value, which might be due to compounds formation among PbO, Al_2O_3 and SiO_2, such as binary compounds of $PbAl_2O_4$ and $PbAl_{12}O_{19}$ as well as ternary compounds of $PbAl_2Si_2O_8$ and $Pb_3Al_{10}SiO_{20}$ (Chen et al., 2001).

CONCLUSIONS

The distribution behaviour of Pb between slag and copper was investigated at 1300 °C and varied pO2 of 10-10 to10-6 atm. For all three slags of FeOx–SiO2 (F slag), CaO–FeOx (CF slag), and FeOx–CaO–SiO2 (FCS slag), the logarithmic distribution ratio increased linearly with an increasing pO2. The distribution ratios in the acidic F slag were much higher than the alkaline CF slag due to the alkaline nature of PbO while FCS slag had a Pb capacity in between. The calculated activity coefficient of PbO in three slags followed the order of CF (1.70) > FCS (0.71) > F (0.44) which were comparable to previous studies. Differences in the Pb distribution ratio and activity coefficient of PbO between the present work and previous studies were observed possibly due to the different crucible, slag composition, possible presence of solids (e.g., olivine) in slag, and operation conditions. Present study suggested that the FCS slag is a suitable substitute for F and CF slags for reducing smelting and oxidising converting during secondary e-waste smelting. A higher (CaO+MgO)/SiO2 mass ratio (when MgO refractory is used) could adversely affect the Pb segregation from copper phase. The variation of Fe/SiO2 mass ratio in the FCS slag didn’t exert significant effects on the Pb distribution ratio and the activity coefficient of PbO.

ACKNOWLEDGEMENTS

Authors are thankful for the financial support and paper submission approval from Mineral Resources, CSIRO. Authors also would like to express thanks to Tom Austin for technical support of experiments, Steve Peacock from CSIRO Mineral Processing for XRF analysis as well as Chris Sheedy and team members from CSIRO Manufacturing for ICP-OES/MS analyses.

REFERENCES

Babu, B R, Parande, A K, and Basha, C A, 2007. Electrical and electronic waste: a global environmental problem. Waste Management & Research, 25(4): 307-318.

Baldé, C, Forti, V, Gray, V, Kuehr, R, and Stegmann, P, 2017. The Global E-waste Monitor 2017: Quantities, Flows, and Resources.

Botor, J, Czernecki, J, and Zajączkowski, A, 2000. Distribution of Cu and Pb between copper alloys and flash smelting slag. Seetharaman S, Sichen Du, Proceedings of the Sixth International Conference on Molten Slags, Fluxes, and Salts, Sztokholm, Sweden-Helsinki, Finland, Sweden: Division of Metallurgy, KTH.,

Chakraborty, S C, Qamruzzaman, M, Zaman, M W U, Alam, M M, Hossain, M D, Pramanik, B K, Nguyen, L N, Nghiem, L D, Ahmed, M F, Zhou, J L, Mondal, M I H, Hossain, M A, Johir, M A H, Ahmed, M B, Sithi, J A, Zargar, M, and Moni, M A, 2022. Metals in e-waste: Occurrence, fate, impacts and remediation technologies. Process Safety and Environmental Protection, 162: 230-252.

Chen, M, Avarmaa, K, Taskinen, P, Klemettinen, L, Michallik, R, O'Brien, H, and Jokilaakso, A, 2021. Handling trace elements in WEEE recycling through copper smelting-an experimental and thermodynamic study. Minerals Engineering, 173: 107189.

Chen, S, Zhao, B, Hayes, P C, and Jak, E, 2001. Experimental study of phase equilibria in the PbO-Al2O3-SiO2 system. Metallurgical and Materials Transactions B, 32(6): 997-1005.

Davenport, W G, King, M J, Schlesinger, M E, and Biswas, A K, 2002. Extractive metallurgy of copper. Elsevier.

Ebin, B, and Isik, M I, 2016. Pyrometallurgical Processes for the Recovery of Metals from WEEE. In A. Chagnes, G. Cote, C. Ekberg, M. Nilsson, & T. Retegan (Eds.), WEEE Recycling (pp. 107-137). Elsevier.

Eerola, H, Jylha, K, and Taskinen, P, 1984. Thermodynamics of impurities in calcium ferrite slags in copper fire-refining conditions. Trans Inst Min Metall, 93: 193-199.

Forti, V, Baldé, C P, Kuehr, R, and Bel, G. (2020). The Global E-waste Monitor 2020: Quantities, flows, and the circular economy potential. Retrieved 02 June from https://ewastemonitor.info/wp-content/uploads/2020/11/GEM_2020_def_july1_low.pdf

Ghodrat, M, Rhamdhani, M A, Brooks, G, Masood, S, and Corder, G, 2016. Techno economic analysis of electronic waste processing through black copper smelting route. Journal of Cleaner Production, 126: 178-190.

Ghodrat, M, Rhamdhani, M A, Khaliq, A, Brooks, G, and Samali, B, 2018. Thermodynamic analysis of metals recycling out of waste printed circuit board through secondary copper smelting. Journal of Material Cycles and Waste Management, 20(1): 386-401.

Hagelüken, C, Umicore, A, and Co, K, 2006. Improving metal returns and eco-efficiency in electronics recycling.

Heo, J, and Park, S, 2012. Effect of Slag Composition on the Distribution Behavior of Pb between FetO-SiO2 (-CaO, Al2O3) Slag and Molten Copper. Metallurgical and Materials Transactions B, 43.

Hidayat, T, Chen, J, Hayes, P C, and Jak, E, 2021. Distributions of As, Pb, Sn and Zn as minor elements between iron silicate slag and copper in equilibrium with tridymite in the Cu–Fe–O–Si system. International Journal of Materials Research, 112(3): 178-188.

Islam, M K, Haque, N, and Somerville, M A, 2021, 2021//. Characterisation and Techno-Economics of a Process to Recover Value from E-waste Materials. TMS 2021 150th Annual Meeting & Exhibition Supplemental Proceedings, Cham.

Islam, M T, and Huda, N, 2019. E-waste in Australia: Generation estimation and untapped material recovery and revenue potential. Journal of Cleaner Production, 237: 117787.

Kaur, R R, Swinbourne, D R, and Nexhip, C, 2009. Nickel, lead and antimony distributions between ferrous calcium silicate slag and copper at 1300°C. Mineral Processing and Extractive Metallurgy, 118(2): 65-72.

Khaliq, A, Rhamdhani, M A, Brooks, G, and Masood, S, 2014. Metal Extraction Processes for Electronic Waste and Existing Industrial Routes: A Review and Australian Perspective. Resources, 3(1): 152-179.

Kim, H G, and Sohn, H Y, 1998. Effects of CaO, Al2O3, and MgO additions on the copper solubility, ferric/ferrous ratio, and minor-element behavior of iron-silicate slags. Metallurgical and Materials Transactions B-Process Metallurgy and Materials Processing Science, 29(3): 583-590.

Kuxmann, U, and Fischer, P, 1974. Beitrag zur Kenntnis der Zustandsdiagramme PbO-Al2O3, PbO-CaO und PbO-SiO2.

Matsuzaki, K, Ishikawa, T, Tsukada, T, and Ito, K, 2000. Distribution equilibria of Pb and Cu between CaO-SiO2-Al2O3 melts and liquid copper. Metallurgical and Materials Transactions B, 31(6): 1261-1266.

Nagamori, M, Mackey, P J, and Tarassoff, P, 1975. Copper solubility in FeO−Fe2O3−SiO2−Al2O3 slag and distribution equilibria of Pb, Bi, Sb and As between slag and metallic copper. Metallurgical Transactions B, 6(2): 295-301.

Nakajima, K, Takeda, O, Miki, T, Matsubae, K, and Nagasaka, T, 2011. Thermodynamic Analysis for the Controllability of Elements in the Recycling Process of Metals. Environmental Science & Technology, 45(11): 4929-4936.

Nithya, R, Sivasankari, C, and Thirunavukkarasu, A, 2021. Electronic waste generation, regulation and metal recovery: a review. Environmental Chemistry Letters, 19(2): 1347-1368.

Shuva, M A H, Rhamdhani, M A, Brooks, G A, Masood, S, and Reuter, M A, 2016. Thermodynamics data of valuable elements relevant to e-waste processing through primary and secondary copper production: a review. Journal of Cleaner Production, 131: 795-809.

Sineva, S, Shishin, D, Starykh, R, Hayes, P C, and Jak, E, 2021. Equilibrium Distributions of Pb, Bi, and Ag between Fayalite Slag and Copper-Rich Metal, Calcium Ferrite Slag and Copper-Rich Metal. Thermodynamic Assessment and Experimental Study at 1250 °C. Journal of Sustainable Metallurgy, 7(2): 569-582.

Takeda, Y, Ishiwata, S, and Yazawa, A, 1983. Distribution Equilibria of Minor Elements between Liquid Copper and Calcium Ferrite Slag. Transactions of the Japan Institute of Metals, 24(7): 518-528.

Takeda, Y, Ishiwata, S, and Yazawa, A, 1984. Distribution of Minor Elements between Slag and Metallic Copper: Equilibrium Study on Calcium Ferrite slags (4th Report). Journal of the Mining and Metallurgical Institute of Japan, 100(1152): 103-108.

Takeda, Y, and Yazawa, A, 1989. Dissolution Loss of Copper, Tin and Lead in FeO sub n--SiO sub 2--CaO Slag. In M. K. a. J. C. Taylor (Ed.), Productivity and technology in the metallurgical industries (pp. 227-240). The Minerals, Metals & Materials Society.

Taskinen, P, and Avarmaa, K, 2021. Simulation of Slag–Matte/Metal Equilibria for Complex and Low-Grade Raw Materials. Sustainability, 13(22): 12826.

Tian, H, Guo, Z, Pan, J, Zhu, D, Yang, C, Xue, Y, Li, S, and Wang, D, 2021. Comprehensive review on metallurgical recycling and cleaning of copper slag. Resources, Conservation and Recycling, 168: 105366.

Yamasue, E, Minamino, R, Numata, T, Nakajima, K, Murakami, S, Daigo, I, Hashimoto, S, Okumura, H, and Ishihara, K N, 2009. Novel Evaluation Method of Elemental Recyclability from Urban Mine —Concept of Urban Ore TMR&mdash. MATERIALS TRANSACTIONS, 50(6): 1536-1540.
Yazawa, A, 1994, 6–8 June 1994. Thermodynamic Interpretation on Oxidic Dissoluton of Metal in Slag. Australian Asian Pacific Course and Conference - Pyrometallurgy for Complex Materials and Wastes, Melbourne, Australia.
Yazawa, A, and Takeda, Y, 1982. Equilibrium Relations between Liquid Copper and Calcium Ferrite Slag. Transactions of the Japan Institute of Metals, 23(6): 328-333.
Ye, F C, Liu, Z H, and Xia, L G, 2021. Materials and Energy Balance of E-Waste Smelting-An Industrial Case Study in China. Metals, 11(11): 1814.